[15]See, for example, Refs. 1 and 5. A very good discussion of this point is given by Kliewer and Fuchs (Ref. 5).

[16]$\hat{y}\times\vec{k}_T=(\tau,0,k_x)$.

[17]Forstmann (Ref. 4) solved these equations approximately. If terms proportional to $(v_F/c)^2$ or kv_F/ω are neglected when compared to unity, we find

$$\frac{B}{A}=-\frac{2Kv_z^2}{(\omega+i\gamma)^2}=-\frac{3\omega_p^2}{2\pi(\omega+i\gamma)^2}\left(\frac{v_z}{v_F}\right)^2$$

for specular scattering, i.e., $p=1$.

[18]See, for example, the Appendix of Ref. 1.

[19]The dispersion relation in the bounded case can be shown to be $\epsilon_L'=-i\gamma/\omega$, i.e., $\mathrm{Re}(\epsilon_L')=0$ and $\mathrm{Im}(\epsilon_L')=-\gamma/\omega$. Since the dispersion is primarily determined by the real part, the imaginary part being associated with the damping length $\mathrm{Im}(k_L)^{-1}$, the boundary has a larger effect on the damping of the longitudinal wave than on its dispersion relation.

PHYSICAL REVIEW B VOLUME 2, NUMBER 4 15 AUGUST 1970

Resistivity of Some *CuAu*Fe Alloys†

J. W. Loram, T. E. Whall, and P. J. Ford
School of Mathematical and Physical Sciences, University of Sussex, Brighton, United Kingdom
(Received 26 January 1970)

The electrical resistivity of a series of *CuAu*Fe alloys, containing 0, 5, 10, and 100 at. % Au, has been measured over the temperature range 0.5–300 °K, and the results are compared with recent theoretical predictions of the resistance anomaly associated with the formation of the spin-compensated state. From such a comparison, the Kondo temperature T_K is found to decrease rapidly with increasing Au concentration from 24 °K in *Cu*Fe to 0.24 °K in *Au*Fe. Although a dependence of the form

$$A-B(T/T_K)^2\ln(T/T_K)^2$$

is found to fit the results of the *CuAu*Fe alloys over a wide range of temperatures, this does not describe the *Cu*Fe results in the low-temperature limit, where a parabolic dependence $C-D(T/T_K)^2$ is observed for $T/T_K<0.06$. An expression of the form

$$E-F\left(1+\frac{S(S+1)\pi^2}{[\ln(T/T_K)]^2}\right)^{-1/2}$$

describes the Au results and those of the *CuAu*Fe alloys at $T>T_K$ with the spin $S=0.77\pm0.25$ if suitable corrections are made for deviations from Matthiessen's rule in the temperature region where phonon scattering is significant.

I. INTRODUCTION

Following the demonstration by Kondo[1] of a logarithmic divergence in the exchange scattering of conduction electrons by magnetic impurities in metals, it was soon realized that strong spin correlations must exist between the conduction electrons in the region of the magnetic impurity at temperatures below the Kondo temperature T_K. For an antiferromagnetic exchange coupling J between the conduction electrons and the localized moment, the Kondo temperature of the system is given by $T_K\sim E_F e^{-1/Jn(E_F)}$, where $n(E_F)$ is the density of states at the Fermi energy E_F. Several authors[2,3] have suggested that as $T\to0$, the conduction electrons are polarized around the impurity in such a way as to completely compensate its magnetic moment. Physically, it may be expected that these correlations will be destroyed by temperatures or magnetic fields comparable with the correlation energy kT_K. Experimental estimates of T_K range from below 10^{-6} °K in *Au*Mn[4] to 300 °K in *Au*V,[5] this variation being consistent with less than an order-of-magnitude change in J.

Theoretical attention has been focused both on the nature of the spin correlations below T_K and on the physical properties of the state as a function of temperature and magnetic field.[6] Expressions have been derived for the temperature dependence of the resistivity above T_K,[1,7] below T_K,[2,8,9] and throughout the entire temperature range.[10,11] The qualitative features of these expressions are similar, predicting that the resistivity due to s-d exchange scattering decreases from the unitarity limit at $T=0$ to a high-temperature plateau proportional to $J^2S(S+1)$ at temperatures far above T_K. (S is the impurity spin.) No discontinuity occurs at T_K, the

transition being spread over several decades in temperature above and below T_K. There is, however, considerable disagreement as to the temperature dependence of the resistivity below T_K, which reflects the uncertainties in the nature of the low-lying excitations of the spin-compensated state.

An alternative description[12,13] assumes that at $T=0$ the ground state of the impurity is nonmagnetic. Fluctuations in the spin of the impurity may occur with a characteristic lifetime τ. At temperatures high compared with $1/\tau$, the state exhibits a Curie law susceptibility and a logarithmically decreasing resistance, while at low temperatures the state appears nonmagnetic and the resistance tends to a constant value. The inverse lifetime, therefore, plays an equivalent role in this theory to the Kondo temperature in the s-d exchange model.

To compare theory with experiment it would be desirable to measure the resistivity of a given alloy system throughout the entire transition region. The very large width in temperature of the transition makes this very difficult for two reasons. First, well below T_K, where the resistance is very close to its value at $T=0$, very accurate measurements are needed to resolve the temperature dependence. Such accuracy becomes increasingly more difficult below 1 °K. At higher temperatures, where phonon scattering is significant, the subtraction of the pure-metal resistivity from that of the dilute alloy to obtain the impurity resistivity can lead to considerable errors, as Matthiessen's rule is not well obeyed even for nonmagnetic impurities or defect scattering.[14] Thus, until there is a more detailed understanding of the breakdown of Matthiessen's rule, the temperature dependence of impurity scattering in the phonon region will remain uncertain.

For these reasons it seems unlikely that measurements on a single system will be sufficiently accurate or reliable to establish the temperature dependence over the whole transition. A more promising approach is to examine systems of both high and low Kondo temperatures at temperatures sufficiently low for phonon scattering to be negligible. If, as all current theories suggest, the resistance can be described by a universal function of T/T_K, the temperature dependence in different limited sections of the transition can be established.

In the present investigation resistivity measurements have been made between 0.45 and 300 °K on *Cu*Fe, *Au*Fe, and some *CuAu*Fe alloys. Previous investigations of the low-temperature resistivity of *Cu*Fe[15–17] indicate that its Kondo temperature may be in the region of 16 °K and this is therefore an ideal system for the investigation of the transition region below T_K. The resistivity[18] of *Au*Fe suggests that its Kondo temperature lies below 0.5 °K, and the temperature dependence of the resistivity above T_K is therefore determined in the present measurements. In an attempt to determine whether the resistance can be represented by a universal function of T/T_K, at least for a small variation of T_K, some *CuAu*Fe alloys containing 5 and 10 at. % Au have also been investigated, for which the Kondo temperature might be expected to lie between that of *Cu*Fe and *Au*Fe. Star *et al.*[19] have measured the resistivity of a series of *CuAu*Fe alloys containing 0.02 and 0.15 at. % Fe. They concluded from these results that T_K decreases across the Cu-Au series, and that the effect of Ruderman-Kittel-Kasuya-Yosida (RKKY) interactions are increasingly important, at a given Fe concentration, as T_K decreases. These conclusions are supported by the present results.

II. EXPERIMENTAL DETAILS

Most of the alloys used in the present investigations were prepared from spectroscopically pure Au (estimated Fe content 5 ppm), 99.999% pure Cu and 99.95% pure Fe, all provided by Johnson Matthey and Co.[20] The *Au*Fe alloys were made by induction melting appropriate amounts of pure Au and a Au(0.1 at. % Fe) master alloy in alumina crucibles. After swaging in brass down to 0.15-cm diam, they were drawn through steel dies to a diameter of 0.025 cm. After etching in aqua regia to remove surface contamination, they were given an homogenizing anneal at 900 °C for 6 h *in vacuo*, and quenched rapidly in iced water. The pure Au specimen (No. 2) was prepared in a similar manner. The other Au specimen (No. 1) was prepared from Cominco 99.999% pure Au containing an estimated 0.5 ppm of Fe. After induction melting in a copper-boat levitation furnace the ingot was rolled between plastic sheets to a tape 0.008 cm thick and cut in the form of a strip approximately 2 mm wide and 12 cm long. This specimen was then etched, annealed, and quenched as described above.

The *Cu*Fe alloys were prepared by induction melting appropriate amounts of pure Cu and a Cu(0.1 at. % Fe) master alloy. These were then prepared in the form of tapes as described above, etched in dilute nitric acid, and vacuum annealed at 900 °C for 6 h. They were quenched in iced water as above. Chemical analysis showed that the pure Cu specimen (No. 7) contained a significant amount of Fe (approximately, 13 ppm Fe). This was confirmed by the large residual resistance (0.034 $\mu\Omega$ cm), and the temperature depen-

dence of the low-temperature resistance (see Sec. III B), which indicates an iron concentration of approximately 15 ppm Fe.

Master alloys of $Cu_{95}Au_5$ and $Cu_{95}Au_5$(0.2 at.% Fe) were prepared and appropriate amounts of these were used in the preparation of the $Cu_{95}Au_5$-Fe alloys. These alloys were induction melted in alumina crucibles and tipped onto a water-cooled copper hearth to prevent segregation of the Cu and Au. The ingots were rolled into strips and given a heat treatment identical to that of the *Cu*Fe alloys. Electron-milliprobe examination showed that segregation was negligible. Chemical analysis (Table II) confirmed that the Au concentration was almost identical in each of the alloys, and that the Fe content was close to the nominal Fe concentration. Residual resistance values are consistent with these conclusions.

A very similar procedure was adopted in the preparation of the $Cu_{90}Au_{10}$-Fe alloys, though more difficulty was experienced in preventing segregation. Examination by means of the electron milliprobe revealed that the specimens selected for resistivity measurements did not show significant segration, but chemical analysis indicated that the Au concentration varied somewhat between specimens (Table II). The Fe concentration as determined by chemical analysis was also significantly lower than the nominal Fe concentration in these alloys.

The cryostat was of a conventional design, using a pumped He_4 reservoir to obtain temperatures between 4.2 and 2.2 °K, and a pumped He_3 reservoir to cover the temperature range 2.2–0.45 °K. Temperatures were stabilized to within 1 mdeg below 4 °K and to within 0.5% of the temperature at higher temperatures, using a carbon thermometer as a temperature-sensing element in an ac resistance bridge circuit. The vapor pressure of the refrigerant was used to determine temperatures below 4.2 °K; and above this temperature a constant-volume gas thermometer was employed. He_3 exchange gas surrounded the specimens to ensure good thermal contact with the vapor pressure and gas thermometers attached to the surrounding copper can. Tests were made to ascertain the temperature rise of the specimens due to Joule heating, and the measuring current was chosen in all cases to limit this temperature rise to less than 1 mdeg. Corrections were made for the Kapitza boundary resistance and thermomolecular pressure difference below 0.7 °K, and appropriate gas thermometer corrections were applied above 4 °K. The uncertainty in temperature below 4 °K does not exceed 4 mdeg. Above 4 °K it is always less than 0.5% of the temperature, and over much of the range it is considerably less than this value. At high temperatures, where the resistance is strongly temperature dependent because of phonon scattering, small differences in temperature between the specimens can lead to significant errors in the difference $\Delta\rho$ between the alloy and pure-metal resistivities. This source of error is minimized in the present apparatus, which holds six specimens (usually five alloys and one pure metal), whose temperatures never differ by more than a few millideg.

Another potentially large source of error in $\Delta\rho$, particularly at high temperatures where $\Delta\rho$ may be a small fraction of the total resistivity, arises from uncertainties in the length/area factor of the specimens. It is difficult to estimate this to better than 2% using direct measuring techniques, and so the following method was employed. The potential knife edges leave small depressions in the specimens. The distance between these depressions is measured with a travelling microscope, and the specimen is then carefully cut at the knife edge marks and weighed accurately. The density is estimated from lattice-spacing data.[21] This allows the length/area of each specimen to be determined to within ±0.3%, even if there is significant irregularity in the cross-sectional area of the specimen.

The resistances of the six specimens were measured potentiometrically using a Tinsley Diesselhorst potentiometer and a photocell galvanometer amplifier as a null detector, allowing reproducible potential measurements to $\pm 10^{-8}$ V. The measuring current was stable to within one part in 10^5 during the time taken to measure the potentials of the six specimens. Resistivity measurements were made at a large number of different temperatures to enable temperature dependences to be established accurately.

III. RESULTS

The resistance anomalies in the Cu-, Au-, and CuAu-based alloys are compared in Fig. 1, where the excess resistance per at.% $\Delta\rho/c$ is plotted against $\log_{10}T$.[22] Each alloy is sufficiently dilute for interactions between impurities to be negligible. Consider first the low-temperature region in which phonon scattering may be neglected (below 15 °K in the *Cu*Fe, and *CuAu*Fe alloys, and below 4 °K in the *Au*Fe alloy). Here the temperature dependence is entirely the result of impurity scattering. None of the curves is linear in $\log_{10}T$ in this temperature range. Assuming that these curves represent different parts of the S-shaped curve which characterizes the transition[10] and that the curvature of the resistance versus $\log_{10}T$ graph is zero at T_K,[11] it is then evident that T_K is below 0.5 °K for *Au*Fe, is in the neighbor-

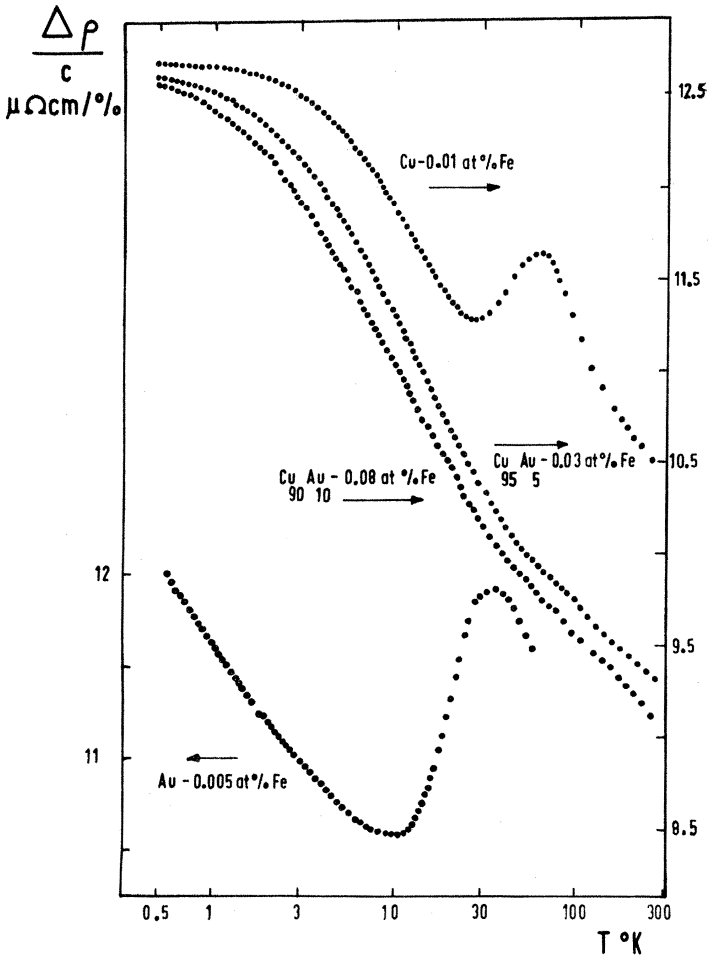

FIG. 1. $(\Delta\rho/c)\mu\Omega$ cm/at. % against $\log_{10}T$ for several *CuAu*Fe alloys.

hood of 10 and 15 °K for $Cu_{95}Au_5$-Fe and $Cu_{90}Au_{10}$-Fe, respectively, and is rather higher for *Cu*Fe. Details of the temperature dependence in this low-temperature region will be discussed below.

At higher temperatures, phonon scattering increases rapidly, and the simple subtraction of the "pure" solvent resistivity from that of the alloy to obtain the impurity resistivity is no longer valid. There is considerable evidence from measurements on nonmagnetic alloys[14] to show that $\Delta\rho$ increases from a low-temperature plateau (the residual resistance) when phonon scattering is negligible, to a higher constant value when phonon scattering dominates. This deviation from Matthiessen's rule originates primarily from the different anisotropies (as a function of conduction electron wave vector) of the phonon and impurity scattering. This problem has received considerable theoretical attention.[23,24] Kohler has shown that the deviation can be expressed as a temperature-dependent correction $\Delta(T)$ to Matthiessen's rule. The total resistivity can be written as

$$\rho = \rho_p + \rho_r + \Delta(T),$$

$$\text{where} \quad \Delta(T) = (1/\gamma\rho_p + 1/\beta\rho_r)^{-1}, \tag{1}$$

ρ_r and ρ_p are the residual resistivity and phonon resistivity, respectively, and β and γ depend on the relative anisotropies of the phonon and impurity scattering and may be temperature dependent. It is evident from Fig. 1 that just such a deviation is occurring in both the Cu(0.01 at.% Fe) and Au(0.005 at. % Fe) alloys, though it is less in evidence in the CuAu-based alloys. Taking ρ_r to be the temperature-dependent impurity resistance, we have shown[25] that Eq. (1) is a fairly good approximation to the observed deviation in a wide variety of dilute magnetic alloys, with β and γ taken to be independent of temperature. γ varies little with alloy system or concentration and has a value of approximately 1.2 ± 0.1 for most of the alloys studied. β, which characterizes the fractional change in the impurity resistance from the low- to high-temperature plateaus, varies approximately as $(0.08 \pm 0.03)\rho_r^{-0.45}$ (ρ_r expressed in

$\mu\Omega$ cm) for residual resistivities in the range 0.02 to 5 $\mu\Omega$ cm. A very large deviation may therefore be expected in the low resistivity Cu(0.01 at. % Fe) and Au(0.005 at. % Fe) alloys and deviations of the order of 15 and 20% of the residual resistance are, in fact, observed in these two alloys.

The deviation in the disordered ternary *CuAuFe* alloy will be the difference in $\Delta(T)$ for the ternary *CuAuFe* alloy and the binary *CuAu* alloy. Using the approximate relation between β and ρ_r mentioned above, the maximum high-temperature deviation may be expected to be of the order of 4% of the Fe *impurity resistivity* in the *CuAuFe* alloys. This rather small deviation is entirely consistent with the measurements on the *CuAuFe* alloys (Figs. 1, 11, and 14) and emphasizes one advantage of making measurements on disordered ternary alloys. The conclusions which can be drawn from the resistance measurements in both the high- and low-temperature regions in each of these systems will be discussed in detail in the following sections.

A. AuFe

In Fig. 2, the total resistivity ρ is plotted against $\log_{10}T$ between 0.5 and 3.5 °K for several very dilute *AuFe* alloys, whose nominal concentrations lie between 0 and 25 ppm Fe. Phonon scattering and effects due to the breakdown of Matthiessen's rule (which varies as $\gamma\rho_p$ at very low temperatures) are negligible in this temperature range, as is evident from the pure Au (specimen 1) results. The positive curvature of the ρ versus $\log_{10}T$ plot is clearly evident in each of the alloys and it results solely from Fe scattering.

Interaction effects are clearly visible in the higher concentration alloys shown in Fig. 3, in which $\Delta\rho/c$ is plotted against $\log_{10}T$ for *AuFe* alloys containing between 0.0025 and 0.04 at. % Fe between 0.5 and 12 °K. The curvature decreases and changes sign at low temperatures, as inelastic scattering processes freeze out in internal fields. The effect occurs at progressively higher temperatures as the concentration increases, and the resistance passes through a maximum at 0.8 °K in the 0.04 at. % Fe alloy. The effects of interactions on the resistance of *AuFe* alloys will be discussed in detail in a later publication.

The curvature in ρ against $\log_{10}T$ for alloys containing 25 ppm and less of Fe (in which interaction effects are assumed to be negligible) allows the temperature dependence to be compared with recent theoretical predictions. The variation of the slope $d\rho/d\log_{10}T$ with temperature is shown in Fig. 4 for the 25 ppm alloy and it can be seen that the slope decreases by a factor of 2 between 0.5 and 4 °K. The rapid decrease in slope above 4 °K is the result of increasing phonon scattering.

Second Born-approximation calculations[1] yield only a term linear in $\log_{10}T$ and cannot describe the observed curvature. Abrikosov[7] has shown that for $T \gg T_K$, the resistivity is proportional to $[\ln(T/T_K)]^{-2}$. This predicts a curvature, but not one which is in accord with experiment, as shown in Fig. 4 (curve A), where T_K has been chosen to be (2×10^{-5}) °K to match the slopes at 0.5 and 4 °K.

Hamann[11] has derived an expression for ρ which should be valid over the entire temperature range from above to below T_K. His expression can be written as

$$\rho = \tfrac{1}{2}\rho_0\{1 \pm [1 + S/(S+1)\pi^2/[\ln(T/T_K)]^2]^{-1/2}\}, \quad (2)$$

where the + sign is to be taken for $T < T_K$ and − for $T > T_K$. $\rho_0 = 4\pi c\hbar/ze^2k_F$ is the s-wave unitarity limit, with c the concentration, z the number of conduction electrons per atom, and k_F the Fermi wave vector. This expression reduces to that due to Abrikosov for $T \gg T_K$. It is readily shown from Eq. (2) that if $Z = d\rho/d\ln T$ is the slope at a temperature T and Z_0 the slope at an arbitrary temperature T_0, then

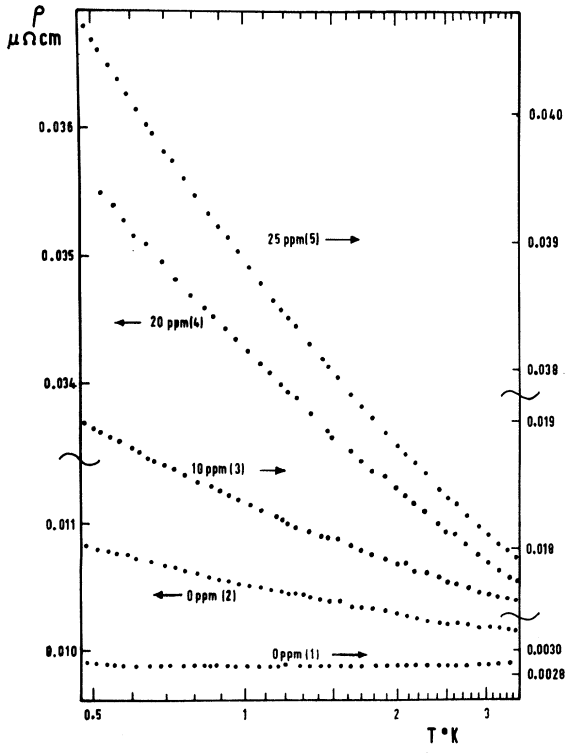

FIG. 2. $\rho\mu\Omega$ cm against $\log_{10}T$ for very dilute *AuFe* alloys. Nominal Fe concentration in each alloy is show in ppm Fe and the specimen number in this and subsequent figures is shown in parentheses.

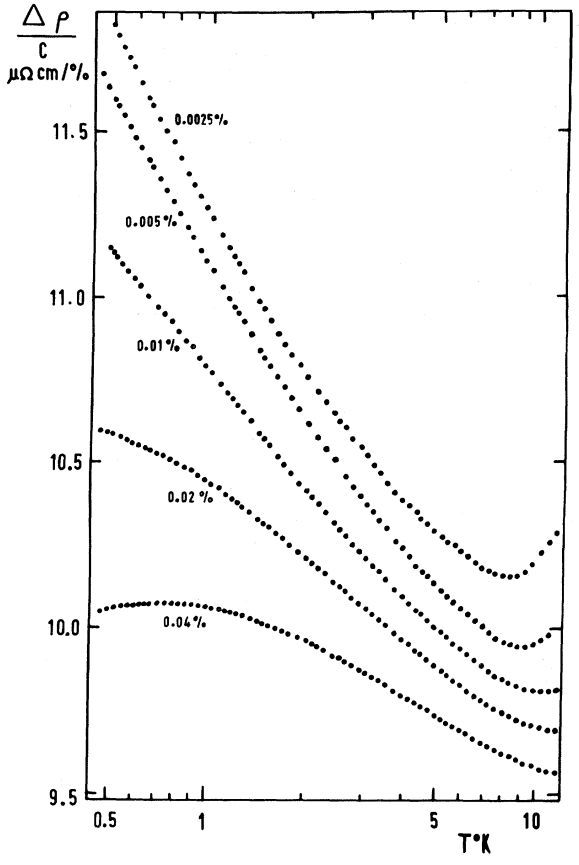

FIG. 3. $(\Delta\rho/c)\mu\Omega$ cm/at. % against $\log_{10}T$ for more concentrated AuFe alloys. Nominal Fe concentration is indicated for each alloy.

$$(n-1)/\ln(T/T_0) = [\ln(T/T_0) - 2\ln(T_K/T_0)] \times \{[\ln(T_0/T_K)]^2 + S(S+1)\pi^2\}^{-1},$$

where $n = (Z_0/Z)^{2/3}$. A plot of $(n-1)/\log_{10}(T/T_0)$ against $\log_{10}(T/T_0)$ should be linear if Eq. (2) is correct. The intercept $-2\log_{10}(T_K/T_0)$ yields the Kondo temperature, and the spin value S can be obtained from the slope. Figure 5 shows such a plot for the 25 ppm alloy taking $T_0 = 1$ °K. A best fit to the points for $T < 3.5$ °K yields $T_K = (0.24 \pm 0.17)$ °K and $S = 0.77 \pm 0.25$. The effects of the breakdown of Matthiessen's rule are apparent above 4 °K.

The scatter in the results of the more dilute alloys does not permit a similar analysis, but their consistency with the Hamann expression with the same values of S and T_K can be demonstrated as follows: If the resistivity can be written as

$$\rho = A + \tfrac{1}{2}BF(T), \tag{3a}$$

where

$$F(T) = 1 - \{1 + 13.5/[\ln(T/0.24\,^\circ\mathrm{K})]^2\}^{-1/2} \tag{3b}$$

is the temperature-dependent part of Eq. (2) appropriate to a spin of 0.77 and $T_K = 0.24$ °K, and A describes the temperature-independent contribution from potential scattering from the iron and from other nonmagnetic impurities, then a plot of ρ against $F(T)$ should be linear. Such a plot for the alloys containing 25 ppm and less of Fe is shown in Fig. 6, and it is seen that linearity is excellent in all cases at temperatures below 3.5 °K where phonon scattering is negligible. It is shown in Ref. 25 that the deviation from this expression at higher temperatures is consistent with the Kohler correction to Matthiessen's rule described by Eq. (1).

The constant term A can be obtained by extrapolating ρ against $F(T)$ to $F(T) = 0$ (i.e., to $T = \infty$) and the coefficient B can be obtained from the slope. Values of A and B for the very dilute AuFe alloys are shown in Table I. Although these quantities can be estimated rather accurately, the magnitudes per at. % Fe are more difficult to estimate. This is because of the rather large fractional uncertainty in the Fe concentration, and the unknown amount of nonmagnetic impurity and defect scattering in the specimens. However, a plot of A and B against the chemically analyzed Fe concentration yields the values $A/c = 9 \pm 2$ $\mu\Omega$ cm/at. % and $B/c = 5.6 \pm 1.0$ $\mu\Omega$ cm/at. %.

Hamann's expression can be modified[26] to include the effect of potential scattering by the inclusion of a single potential phase shift δ_v. Equation (2) then becomes

$$\rho = \rho_0 \sin^2\delta_v + \tfrac{1}{2}\rho_0 \cos 2\delta_v F(T) .$$

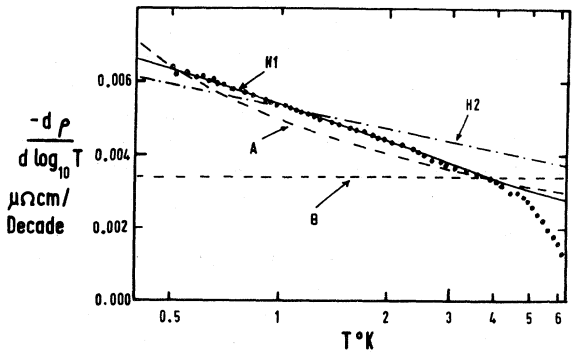

FIG. 4. $-d\rho/d\log_{10}T$ against $\log_{10}T$ for the Au(0.0025 at. % Fe) alloy. Variation of $-d\rho/d\log_{10}T$ as predicted by a second Born-approximation calculation (B), Abrikosov's expression with $T_K = 2\times10^{-5}$ °K (A), and Hamann functions with $T_K = 0.24$, $S = 0.77$ (H1) and $T_K = 0.1$ °K, $S = 1.3$ (H2) are indicated in the figure.

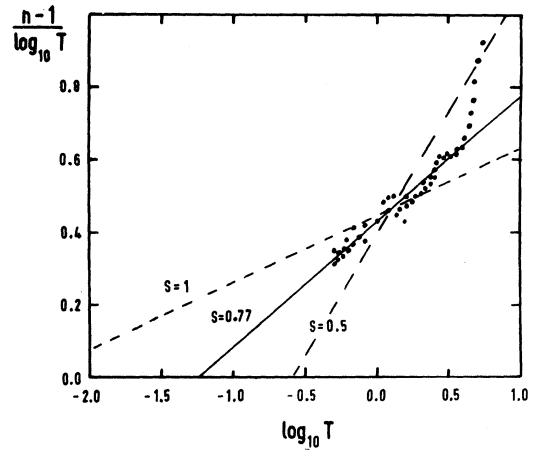

FIG. 5. $(n-1)/\log_{10}T$ against $\log_{10}T$ for the Au (0.0025 at. % Fe) alloy. Linear variation predicted by Eq. (2) for spin values $S=0.5$, 0.77, and 1.0 is also shown.

Taking the present values of A/c $(=\rho_0 \sin^2\delta_v)$ and B/c $(=\rho_0 \cos 2\delta_v)$, we find that $\sin\delta_v = 0.62$ and $\rho_0 = 23.5$ $\mu\Omega$cm/at. %. This value for ρ_0 is in good agreement with the unitarity limit for d-wave scattering in Au (21.5 $\mu\Omega$cm/at. %).

B. CuFe

In Fig. 7 the excess resistivity per at. % $\Delta\rho/c$ is plotted against $\log_{10}T$ between 0.5 and 300 °K for two *Cu*Fe alloys containing nominally 0.01 and 0.04 at. % Fe. The total resistivity of the pure Cu specimen (containing an estimated 15 ppm Fe) is also included. The resistance is linear in $\log_{10}T$ over the rather narrow temperature range between 10 and 20 °K, and flattens off at both higher and lower temperatures. The flattening at low temperatures is comparable for all three specimens and is therefore not a result of magnetic ordering. As was first pointed out by Daybell and Steyert,[17] this behavior results from the spin compensation of the Fe impurities. They estimated the Kondo temperature of the *Cu*Fe system to be of the order of 16 °K from their measurements.

At high temperatures the excess resistance passes through a minimum at around 30 °K followed by a maximum at around 70 °K, and tends at the highest temperatures to a logarithmic temperature dependence which is displaced vertically from the continuation of the low-temperature logarithmic slope. As described above, this behavior results from the breakdown of Mattheissen's rule, and the effect of applying a Kohler correction [Eq. (1)] with $\beta = 0.14$ and $\gamma = 1.0$ to the Cu (0.04 at. % Fe) resistance curve is shown by the dashed curve in Fig. 7. Although these values of β and γ are consistent with values found in other dilute alloys, the correction is too large to allow the impurity resistance at high temperature to be known with confidence. An additional source of uncertainty comes from error in the length/area factor for the specimen. A combined error of $\pm 0.2\%$ in this factor in the pure Cu and *Cu*Fe specimen is shown at several temperatures by vertical bars. The results do suggest, however, that the resistance of *Cu*Fe may be varying logarithmically up to at least 300 °K. This is in contrast to the conclusions of Daybell and Steyert,[17] who assumed that the impurity resistance became temperature independent above 30 °K. We therefore find a larger step height $[\rho(T=0) - \rho(T=\infty)]$, and a broader transition than has been found previously, although it is not possible to deduce either of these quantities with confidence.

The flattening of $\Delta\rho$ versus $\log_{10}T$ at low temperatures superficially resembles the behavior of the Hamann function below T_K. However, an examination of Fig. 8 in which the excess resistance $\Delta\rho$ is plotted against T shows that the low-temperature resistance is not well described by this relation. The negative slope of the Hamann func-

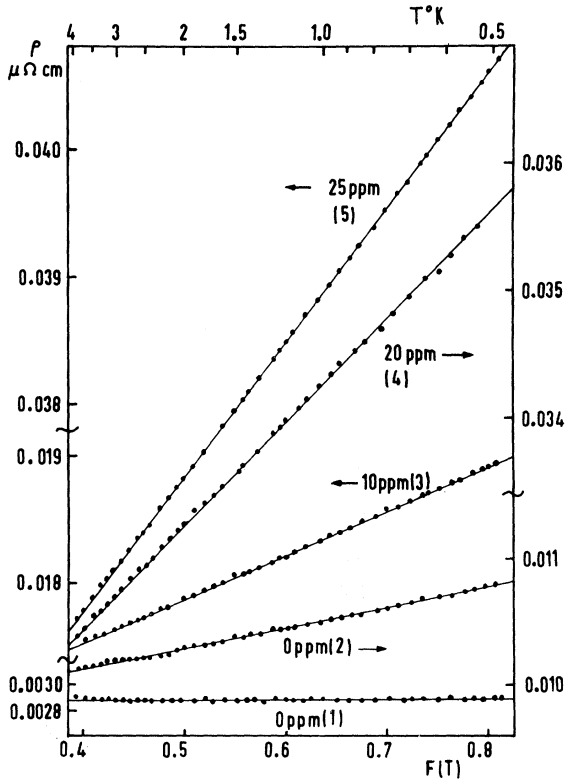

FIG. 6. $\rho\mu\Omega$cm against $F(T)$ [defined by Eq. (3b)] for the very dilute *Au*Fe alloys.

TABLE I. Concentrations and values of coefficients A and B for very dilute AuFe alloys.

Specimen No.	Nominal Fe concentration (ppm)	Analyzed Fe concentration (ppm)	ρ(1 °K) $\mu\Omega$ cm	A $\mu\Omega$ cm	B $\mu\Omega$ cm
1	0	5	0.0029	0.0029	0.0005
2	0	10	0.0105	0.0094	0.0034
3	10	10	0.0182	0.0160	0.0070
4	20	28	0.0343	0.0291	0.0162
5	25	37	0.0388	0.0321	0.0210

tion diverges logarithmically as $T \to 0$, whereas the present results, and the results of previous investigations of this system, [15–17] show that the slope decreases at $T \to 0$. It has been suggested[17] that in this low-temperature region the results fit the dependence predicted by Nagaoka[2]:

$$\rho = \rho_0[1 + \tfrac{1}{3}\pi^2(T/\Delta)^2]^{-1} \quad \text{for } T < T_K\,, \tag{4a}$$

$$\rho = \rho_0[1 - 4.28(T/T_K)^2] \quad \text{for } T < 0.2\,T_K\,, \tag{4b}$$

where Δ is the temperature-dependent width of the resonance, and is equal to 0.88 T_K at $T = 0$. An identical expression has been obtained by Klein, [9] and a parabolic dependence similar to Eq. (4b) has been derived by Levine *et al.* [12] and by Rivier and Zuckermann[13] on the basis of a spin-fluctuation model. To compare this dependence with the CuFe results we plot in Fig. 9 the resistance ρ against T^2. A T^2 dependence is consistent with the results below 1.0 °K for the Cu (0.04 at. % Fe) alloy and below 1.3 °K for the two

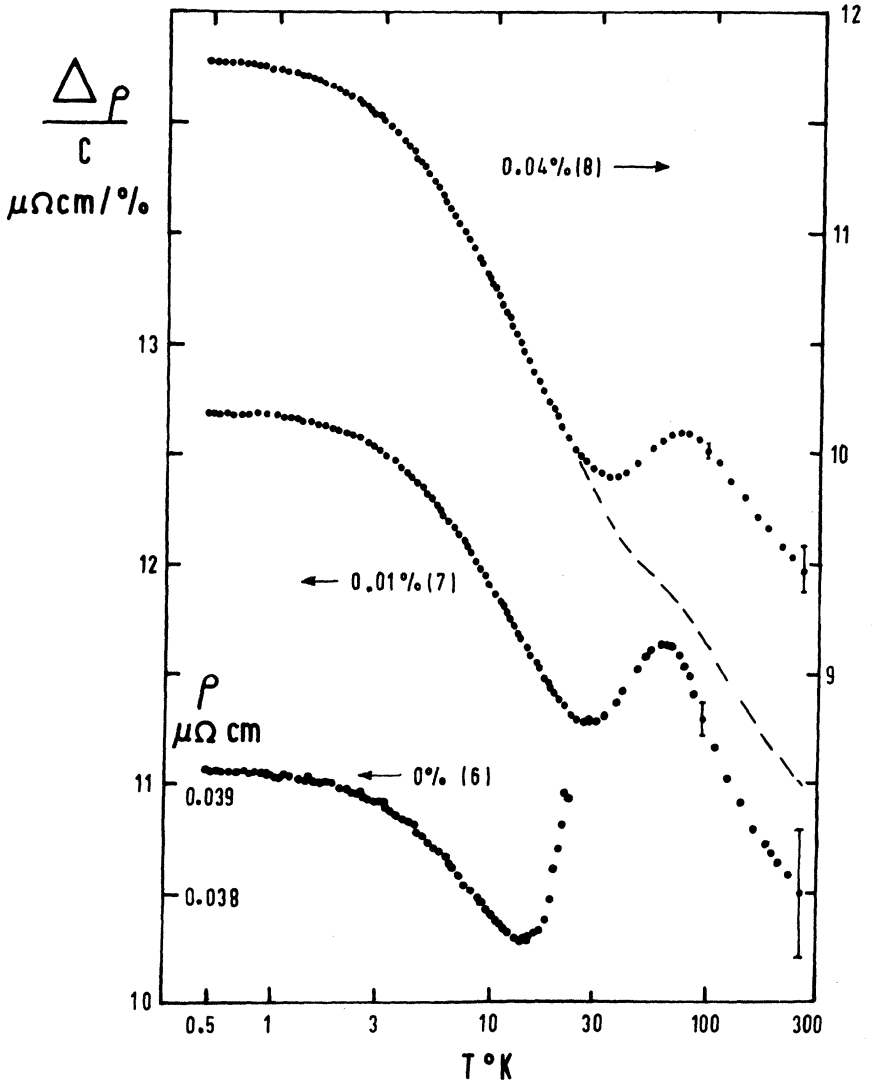

FIG. 7. $\rho\mu\Omega$cm against $\log_{10}T$ for the pure Cu specimen and $\Delta\rho/c\mu\Omega$cm/at. % against $\log_{10}T$ for the two CuFe alloys. (Note the different resistivity scales.) The error bars represent an uncertainty of ±0.2% in the length/area factor of each alloy. The dashed line indicates results for the Cu (0.04 at. % Fe) alloy corrected for the deviation from Mattiessen's rule.

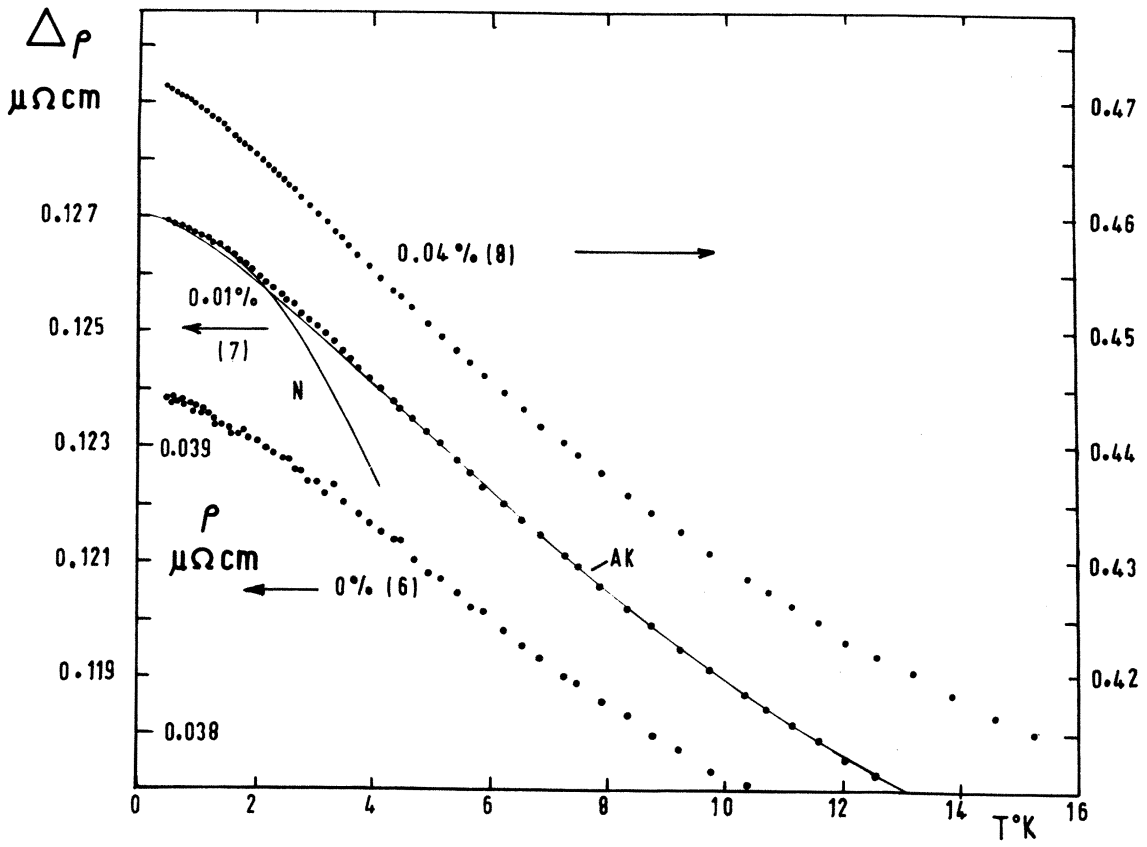

FIG. 8. $\rho\mu\Omega$cm against T for the pure Cu specimen and $\Delta\rho\mu\Omega$cm against T for two *Cu*Fe alloys. (Note different resistivity scales.) Nagaoka expression [Eq. (4a)] with $T_K = 24$ °K, and the Appelbaum-Kondo expression [Eq. (5)] with $T_K = 56$ °K, are shown by the lines labeled N and AK, respectively, and are compared with the results for the Cu(0.01 at. % Fe) alloy.

more dilute alloys. Measurements by Star and Nieuwenhuys[27] on a Cu(0.0055 at. % Fe) alloy demonstrate that the T^2 law is obeyed down to 0.1 °K. The initial slope of the ρ-T^2 plot is, from (4b), given by $4.28\rho_0/T_K^2$, and assuming ρ_0 to be the step height $\rho(T=0) - \rho(T=\infty)$, we can estimate T_K. An examination of Fig. 7 indicates a step height of approximately 4 $\mu\Omega$ cm and this yields values of T_K of 24 and 17 °K for the 0.01 and 0.04 at. % alloys, respectively. A comparison of Eq. (4a) with the Cu(0.01 at. % Fe) results is shown in Fig. 8 by the broken line (N) and significant departures are observed above 1.3 °K. Thus, a parabolic dependence describes the results for $T/T_K < 0.06$, whereas Nagaoka's expression predicts such a dependence up to $T/T_K \sim 0.2$.

An alternative expression for the resistivity has been given by Applebaum and Kondo, [8] who find that for $T \ll T_K$,

$$\rho = \rho_0\{\cos^2\delta_v - \tfrac{16}{3}\cos 2\delta_v (T/T_K)^2[\ln(T/T_K)]^2\} \quad , \qquad (5)$$

where δ_v is the phase shift for potential scattering. If this expression is valid, a plot of $[\rho(0)-\rho]^{1/2}/T$ against $\log_{10}T$ [where $\rho(0)$ is the resistance at $T=0$] should be linear, with an intercept on the $\log_{10}T$ axis of $\log_{10}T_K$. Such a plot for the three *Cu*Fe alloys is shown in Fig. 10. While a logarithmic dependence is observed at higher temperatures, $[\rho(0)-\rho]^{1/2}/T$ tends to a constant value below 1 °K, consistent with the parabolic temperature dependence demonstrated in Fig. 9.

A plot of this kind is very sensitive to the choice of $\rho(0)$, though errors due to this cause decrease rapidly with increasing temperature. To indicate the possible magnitude of this uncertainty, error bars are shown in Figs. 10, 13, and 16, which correspond to a ±20% change in the magnitude of $[\rho(0)-\rho]$ at 0.5 °K. In spite of the failure of Eq. (5) to describe the results at the lowest temperatures, the agreement at higher temperatures allows an estimate of T_K to be made, and values obtained in this way are listed in Table II. It is

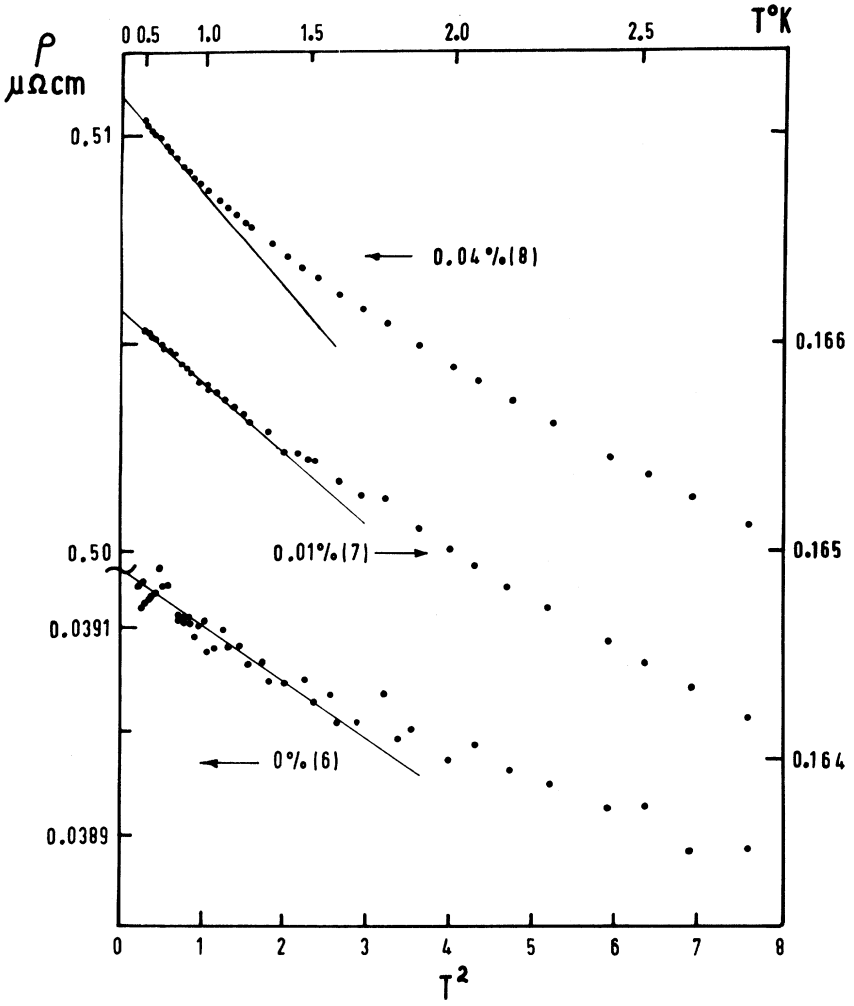

FIG. 9. $\rho\mu\Omega$cm against T^2 for CuFe alloys.

evident that these values of T_K are substantially higher than values obtained from the fit to Eq. (4b). Both methods of determining T_K indicate a slight decrease in T_K with increasing concentration. The slopes D of the curves in the linear region are also listed in Table II.

C. $Cu_{95}Au_5$-Fe

In Fig. 11 we plot $\Delta\rho/c$ against $\log_{10}T$ for four $Cu_{95}Au_5Fe$ alloys, where $\Delta\rho$ is the difference between the resistances of the $Cu_{95}Au_5$-Fe and $Cu_{95}Au_5$ alloys. The general features of the curves at low temperatures are similar to those of the CuFe alloys (Fig. 7). At higher temperatures there is no sign in any of the curves of the minimum- and high-temperature maximum in $\Delta\rho$ which were evident in the CuFe and AuFe alloys. The reasons for the much reduced deviation from Matthiessen's rule in the ternary alloys have already been discussed. The deviation can be estimated, assuming that it is given by the difference between the deviations in the $Cu_{95}Au_5$-Fe and the $Cu_{95}Au_5$ alloys as calculated from Eq. (1). The result of applying this correction to the two most concentrated alloys is shown by the dashed curves in Fig. 11. Although this may not be a completely satisfactory procedure, it serves to indicate the magnitude of the possible error due to this cause. Errors due to a ± 0.2% uncertainty in the length/area factor are shown at several temperatures by vertical bars.

The temperature dependence of $\Delta\rho/c$ at low temperatures is shown in Fig. 12. The pronounced flattening off seen in CuFe is less evident in the $Cu_{95}Au_5$-Fe alloys, suggesting a significantly lower T_K in the latter system. A fit of the resistivity to a T^2 dependence between 0.5 and 0.8 °K yields values of T_K [using Eq. (4b)] of 13 and 11 °K for the $Cu_{95}Au_5$ alloys containing 0.01 and 0.03 at. % Fe, respectively.

Making a suitable choice of $\rho(0)$ the resistance can be seen to fit the Appelbaum-Kondo expression between 0.5 and 5 °K (Fig. 13), though the uncertainty in $\rho(0)$ make it impossible to be certain

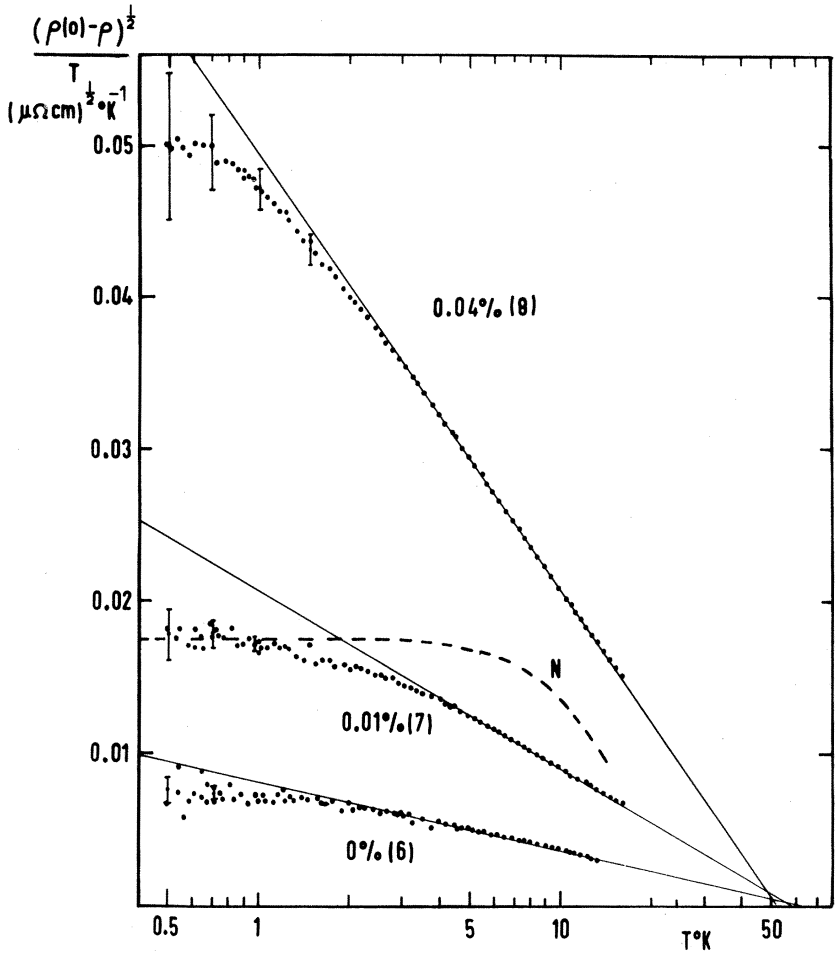

FIG. 10. $[\rho(0)-\rho]^{1/2}/T$ $(\mu\Omega\,\mathrm{cm})^{1/2}\,^{\circ}\mathrm{K}^{-1}$ against $\log_{10}T$ for *Cu*Fe alloys. Solid lines represent the predictions of Eq. (5), and the dashed line (N) the prediction of Nagaoka's expression [Eq. (4a)] with $T_K = 24\,^{\circ}\mathrm{K}$ for the Cu (0.01 at. % Fe) alloy. For a discussion of the error bars, see text.

that $[\rho(0)-\rho]^{1/2}/T$ is not tending to a constant value (i.e., a simple parabolic dependence) at the lowest temperatures (see error bars). The values of T_K found from the intercepts are almost a factor of 2 lower than in the *Cu*Fe system, a quite remarkable decrease for the addition of just 5 at. % of Au. Again the value of T_K is concentration dependent, decreasing with increasing concentration. There is an interesting progression in the temperature dependence with varying Fe concentration to be seen in the results (Fig. 12 As the concentration increases to 0.08 at. % Fe, the low-temperature curvature decreases owing (possibly) to a reduction in T_K (or Δ). With further increase in concentration to 0.2 at. % Fe the curvature increases again, but this time because of incipient ordering of the Fe spins. A fit of Eq. (5) with $T_K = 26\,^{\circ}\mathrm{K}$ to the $Cu_{95}Au_5$ (0.03 at. % Fe) alloy is shown in Fig. 12.

D. $Cu_{90}Au_{10}Fe$

In Fig. 14 we plot $\Delta\rho/c$ against $\log_{10}T$ for the $Cu_{90}Au_{10}$-based alloys. As described in Sec. II the Fe concentration in these alloys was found by chemical analysis to be very much smaller than the nominal concentration. The analyzed concentrations were therefore used in calculating $\Delta\rho/c$. The Au concentration also varied somewhat from alloy to alloy, and a correction has been made for this when estimating the Fe residual resistance. With these sources of uncertainty and the very small contribution of the Fe to the total resistance, the magnitude of $\Delta\rho$ may be in error by a rather large constant amount. The temperature dependence will, however, be unaffected by these uncertainties.

The absence of large deviations from Mattheissen's rule is again apparent. A correction based on the considerations of Sec. III C is shown in Fig. 14 for the $Cu_{90}Au_{10}$ alloys containing 0.2 and 0.08 at. % Fe. Errors due to an uncertainty of $\pm 0.2\%$ in the length/area factor are also shown by the vertical bars.

The low-temperature dependence is shown in

TABLE II. Concentrations, Kondo temperatures, and values of the coefficients D and E for the $CuAu$Fe alloys.

Specimen No.	Alloy	Analyzed Fe concentration (at. %)	Analyzed Au concentration (at. %)	T_K(°K)[a]	T_K(°K)[b]	D $(\mu\Omega\,\mathrm{cm})^{1/2}$	E ($\mu\,\Omega$cm/at. %)[c]
6	Cu	0.0013			59	0.0045	
7	Cu(0.01 at. % Fe)	0.009		24	56	0.0117	1.52
8	Cu(0.04 at. % Fe)	0.040		17	51	0.0288	1.92
9	$Cu_{95}Au_5$	0.0007	4.64				
10	$Cu_{95}Au_5$(0.01 at. % Fe)	0.017	4.65	13	30	0.0213	1.45
11	$Cu_{95}Au_5$(0.03 at. % Fe)	0.036	4.66	11	26	0.0430	1.51
12	$Cu_{95}Au_5$(0.08 at. % Fe)	0.080	4.70		19	0.0805	1.04
13	$Cu_{95}Au_5$(0.2 at. % Fe)	0.19	4.57				
14	$Cu_{90}Au_{10}$	0.0008	8.53				
15	$Cu_{90}Au_{10}$(0.03 at. % Fe)	0.0075	8.81		19	0.0291	1.45
16	$Cu_{90}Au_{10}$(0.08 at. % Fe)	0.0085	8.62		19	0.0325	1.59
17	$Cu_{90}Au_{10}$(0.2 at. % Fe)	0.031	8.93		15	0.0737	1.40

[a]Deduced from Nagaoka's expression Eq. (4b).

[b]Deduced from Appelbaum-Kondo expression Eq. (5).

[c]Step height deduced from Eq. (5); $E=\frac{3}{16}\,c\,(DT_k/2.3)^2 = \rho_0 \cos 2\delta_v$.

Fig. 15 and this is almost linear down to 0.5 °K. This can again be interpreted as a further decrease in T_K. A fit to the Appelbaum-Kondo expression (Fig. 16) is possible up to about 4 °K, making an appropriate choice of $\rho(0)$. The values of T_K obtained from Fig. 16 are lower than those for the $Cu_{95}Au_5$ alloys, and a decrease in T_K with increasing concentration is again apparent.

IV. DISCUSSION

Figure 6 demonstrates clearly that the Hamann expression [Eq. (2)] gives an excellent fit to the resistivity of very dilute AuFe alloys between 0.5 and 4 °K when T_K is chosen to be 0.24 °K and $S = 0.77$. As the spin-dependent scattering has only been determined unambiguously over one decade in temperature, Hamann functions using other values of T_K and S can be found which fit the results almost, though not quite, as well.

Since the curvature $dZ/d\ln T$ is known rather accurately in the neighborhood of 1 °K, an examination of Fig. 5 shows that the possible choices for S and T_K are not independent. In particular, an increase in the value of the spin pushes T_K to lower temperatures with a consequent increase in the step height. For example, a best fit to the results assuming $S = 1.4$ yields $T_K = 10^{-2}$ °K and $B = 15$ $\mu\Omega$ cm/at. %. Values of S greater than 1.2 or less than 0.5 would appear to lie outside the range of experimental error, and this limits T_K to the temperature range $0.04\ ^\circ\mathrm{K} < T_K < 0.5\ ^\circ\mathrm{K}$.

It is interesting to compare the present values of T_K with values obtained from other properties. As with the resistivity, one is forced to make a comparison of a broad experimentally determined feature with a relevant theoretical expression in order to determine T_K. Suhl and Wong[10] have pre-

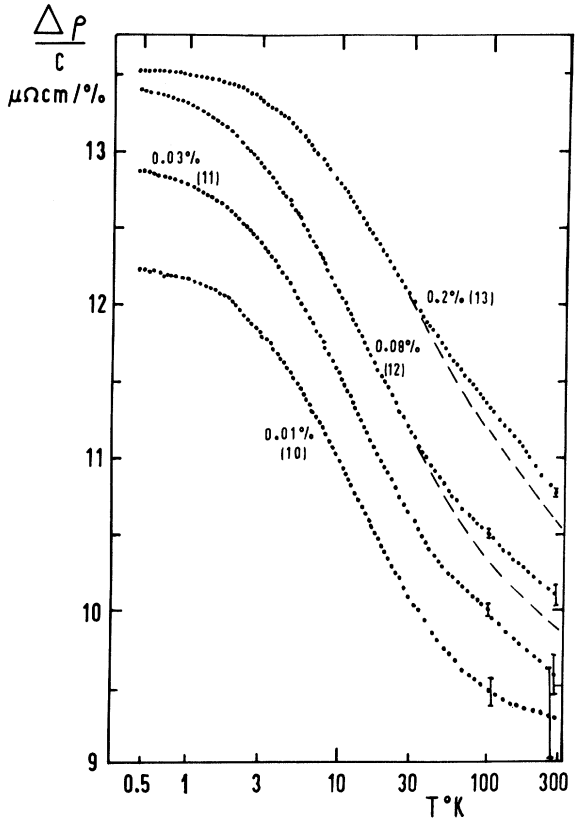

FIG. 11. $(\Delta\rho/c)\mu\Omega$cm/at. % against $\log_{10}T$ for $Cu_{95}Au_5$-Fe alloys. Small vertical displacements (not exceeding 1 $\mu\Omega$cm/at. %) have been made in Figs. 11 and 12 to enable the curves to be clearly distinguished. Error bars represent an uncertainty of ±0.2% in the length/area factor of each specimen. Dashed lines indicate results corrected for deviation from Matthiessen's rule.

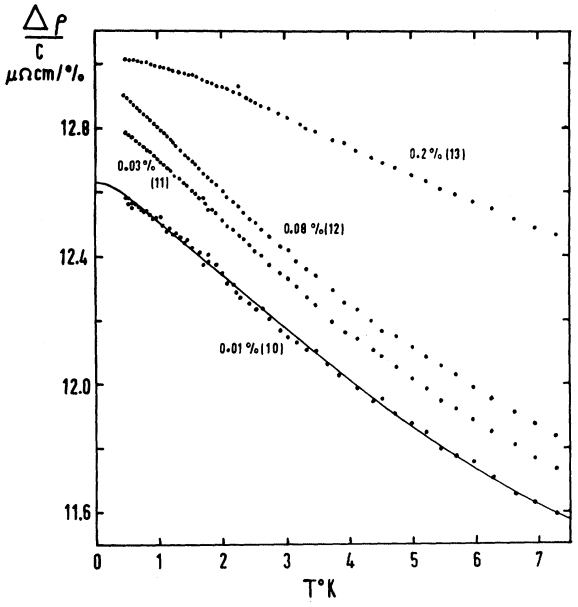

FIG. 12. $(\Delta\rho/c)\mu\Omega$cm/at. % against T for $Cu_{95}Au_5$-Fe alloys. The Appelbaum-Kondo expression [Eq. (5)] with $T_K = 30$ °K (solid line) is compared with the results for the $Cu_{95}Au_5$ (0.01 at. % Fe) alloy.

dicted a maximum in the thermoelectric power at around $T = T_K$, though its position depends somewhat on the magnitude of potential scattering. Nagaoka[2] and Bloomfield and Hamann[28] find that the maximum in the specific-heat anomaly occurs at around $\frac{1}{3}T_K$. If the susceptibility is analyzed in terms of a Curie-Weiss law, the Curie temperature is approximately equal to T_K for $T \ll T_K$ (Klein[9]) and to 4.5 T_K for 10 $T_K < T < 100$ T_K (Scalapino[29]).

Experimentally, the following features are observed. Thermopower measurements on pure Au specimens (in which Fe is the dominant impurity) and on very dilute *Au*Fe alloys[18] indicate that the thermopower of *Au*Fe passes through a broad maximum between 1 and 2 °K. From susceptibility measurements in the range 6–300 °K, Hurd[30] finds a Curie temperature of around 10 °K. Susceptibility measurements by Loram *et al.*[31] in the range 1.5–4.2 °K yield a Curie temperature of 0.5 °K (consistent with $T_K \sim 0.1$ °K[29]). Thus, values of T_K obtained from these properties are in reasonable agreement with that obtained in the present study.

No measurements have been made of the specific heat of *Au*Fe alloys which are sufficiently dilute to avoid interactions and at sufficiently low temperatures to observe the break up of the spin-compensated state. Entropy measurements have been made on more concentrated alloys, in which a magnetic-ordering anomaly is observed, yielding values for the spin on the Fe atoms. Thus, du Chatenie *et al.*[32] finds that $S = 0.65$ for a Au (0.092 at. % Fe) alloy and Potton[33] finds that $S = 0.9 \pm 0.2$ for a Au(0.1 at. % Fe) alloy. Hurd's[30] susceptibility measurements give $S = 1.4$, while a fit of the measurements by Loram *et al.*[31] to Scalapino's formula[29] yields $S = 1.3$ and $T_K = 0.1$ °K. A comparison of the slope of the Hamann expression Eq. (2) (calculated with these values of T_K and S) and the present experimentally determined slopes is shown in Fig. 4 (curve H2), and agreement is poor. A Hamann function with $S = 1.3$ is significantly broader than that observed experi-

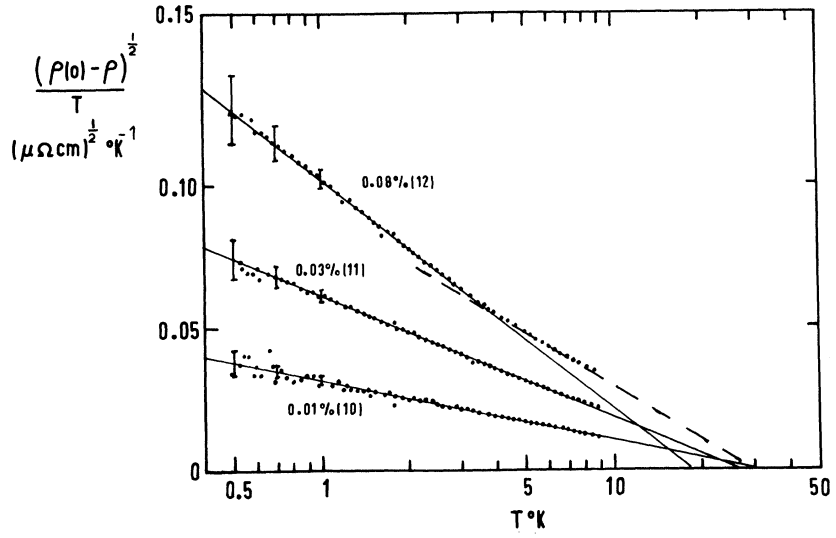

FIG. 13. $[\rho(0) - \rho]^{1/2}/T$ $(\mu\Omega\,\text{cm})^{1/2}\,°\text{K}^{-1}$ against $\log_{10}T$ for $Cu_{95}Au_5$-Fe alloys. For a discussion of error bars, see see text.

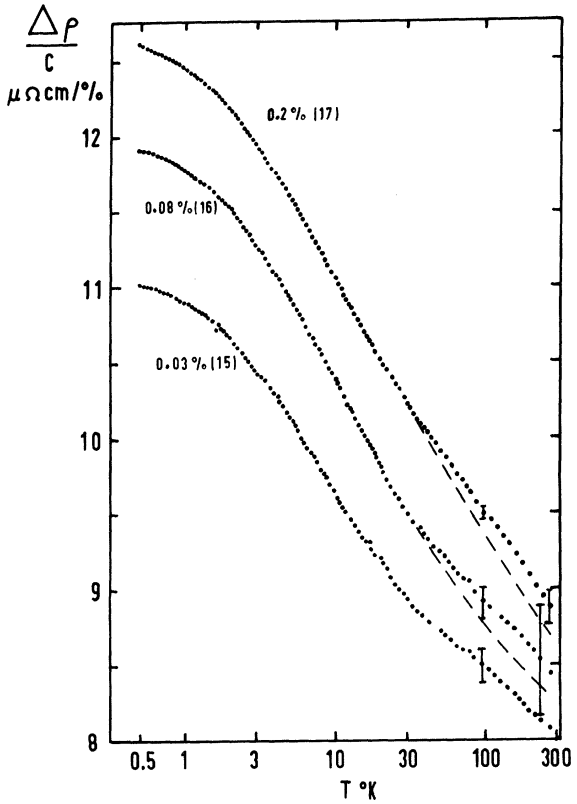

FIG. 14. $(\Delta\rho/c)\mu\Omega$ cm/at. % against $\log_{10}T$ for $Cu_{90}Au_{10}$-Fe alloys. Vertical displacements (not exceeding 3 $\mu\Omega$ cm/at. %) have been made in Figs. 14 and 15. Error bars represent an uncertainty of $\pm 0.2\%$ in the length/area factor of each specimen. Dashed lines indicate results corrected for deviation from Matthiessen's rule.

mentally.

The Hamann expression, which provides an excellent fit in *Au*Fe alloys above T_K does not describe the temperature dependence in the *Cu*Fe and *CuAu*Fe alloys below T_K. Instead, a limiting T^2 dependence fits the *Cu*Fe results at the lowest temperatures, though as an examination of Figs. 10, 13, and 16 reveals, this is valid up to a very much smaller fraction of T_K than is expected on the basis of Eq. (4a). [A comparison of Eq. (4a) with the resistivity of Cu(0.01 at. % Fe) is shown by the dashed line (N) in Fig. 10.]

The Appelbaum-Kondo expression fails to account for the resistivity of *Cu*Fe at very low temperatures, but provides a good fit over an extended temperature range at higher temperatures in all of the *CuAu*Fe alloys. It also yields values for T_K which are more than a factor 2 greater than those obtained from Eq. (4b), and which are significantly higher than the temperature at which $dZ/d\ln T = 0$, that is, T_K defined by Eq. (2).

Values of T_K can also be obtained from other properties of *Cu*Fe. The thermoelectric power passes through a maximum at around 25 °K.[34] Hurd[35] has found that the Curie temperature falls from approximately 32 °K at high temperatures to 15 °K at lower temperatures. The specific heat[36] passes through a broad maximum between 5 and 10 °K. In a careful analysis of Mössbauer and NMR measurements in *Cu*Fe, Golibersuch and Heeger[37] have shown that the quasispin amplitude is reduced to zero in a field of approximately 60 kg or at a temperature of around 20 °K. Thus these properties suggest that T_K lies between 15 and 25 °K in *Cu*Fe. The value of 24 °K obtained from the parabolic temperature dependence, Eq. (4b), is thus in better agreement with these estimates than the value of 50 to 60 °K obtained from the fit to the Appelbaum-Kondo expression Eq. (5).

Two distinct types of concentration dependence are apparent in the present results. These can be characterized by the relative magnitude of T, T_K, and T_{int}, where T_{int} is the mean interaction energy via RKKY spin oscillations between "bare" iron impurities, and is proportional to concentration.

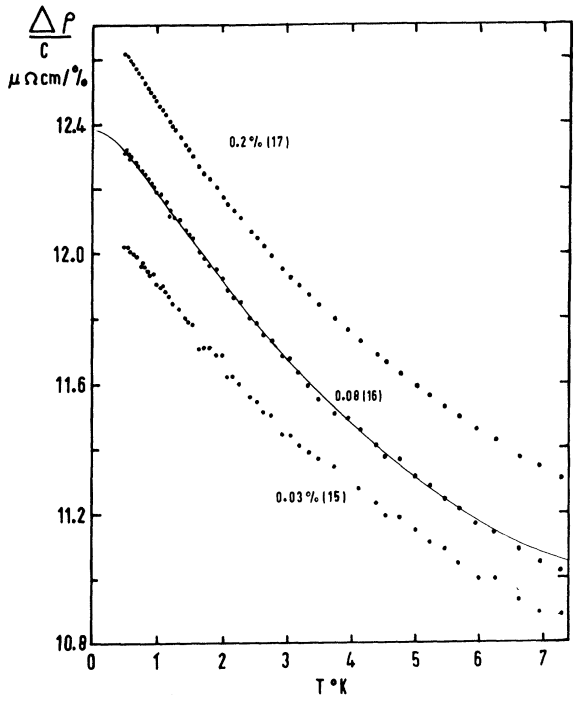

FIG. 15. $(\Delta\rho/c)\mu\Omega$ cm/at. % against T for $Cu_{90}Au_{10}$-Fe alloys. Appelbaum-Kondo expression Eq. (5) with $T_K = 19$ °K (solid line) is compared with the results for the $Cu_{90}Au_{10}$(0.08 at. % Fe) alloy.

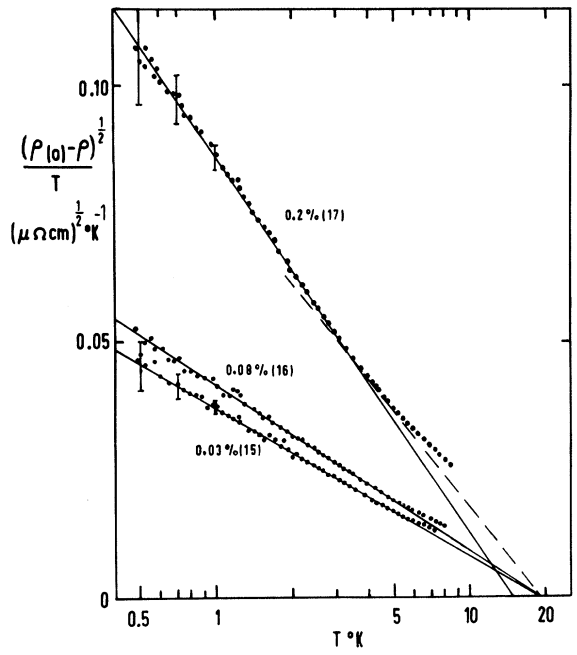

FIG. 16. $[\rho(0)-\rho]^{1/2}/T$ $(\mu\Omega\,\mathrm{cm})^{1/2}\,^{\circ}\mathrm{K}^{-1}$ against $\log_{10}T$ for $Cu_{90}Au_{10}$-Fe alloys. For a discussion of error bars, see text.

1. $T_{\mathrm{int}} > T_K$

The amplitude of the compensating spin cloud is strongly reduced by RKKY interactions when these exceed the binding energy T_K. For $T < T_{\mathrm{int}}$ inelastic spin-flip processes freeze out (as predicted by first Born-approximation calculations[38]) and the slope of the resistance curve decreases. At a temperature of 0.5 °K this is first apparent at $c \sim 0.005$ at. % Fe in *Au*Fe (Fig. 3) and $c \sim 0.2$ at. % Fe in $Cu_{95}Au_5$-Fe (Fig. 12). This is consistent with the very much higher value of T_K in the latter system. This effect is demonstrated in a striking way by the measurements of Star *et al.*[19] on CuAu (0.15 at. % Fe) alloys.

2. $T_{\mathrm{int}} \ll T_K$, $T < T_{\mathrm{int}}$

In this regime the slope of the resistance curve is *increased* by interactions, and this is manifested as an apparent decrease in T_K.[39] A $T > T_{\mathrm{int}}$ [where T_{int} is estimated from *Au*Fe alloys (Fig. 3) of a comparable concentration] the temperature dependence of the resistance is independent of concentration (dashed lines in Figs. 13 and 16). It is not clear whether the interactions causing this effect are due to the overlap and correlation of the long-range compensating spin clouds (Nagaoka[40]) or the RKKY oscillations which are thought to persist below T_K (Suhl[41]).

In terms of a spin-fluctuation model, correlation between the spin fluctuations on several impurities may be expected to increase their lifetime, leading to an increase in the coefficient of the T^2 resistivity at $T < T_{\mathrm{int}}$.[13] (This is just what is observed in the Cu(0.04 at. % Fe) alloy and which we have interpreted as a decrease in T_K.) This would also account for the strong concentration dependence at $T \ll T_K$ of the specific heat of *Cu*Fe.[42]

Figure 17 shows the variation of T_K and J across the series Cu-Au. It is evident that there is a very rapid decrease in J with increasing Au concentration, which falls by a factor of 1.6 across the series. T_K, and hence J, is, in fact, systematically lower in each of the Au–transition-metal alloys compared with the corresponding Cu-based alloys.[43] Because of the similarity of Cu and Au, from a band-structure point of view this difference is not easy to understand.

Star *et al.*[19] have suggested that the decrease in Fermi energy across the series Cu-Au may lead to a narrowing of the virtual state, with, according to the Schrieffer-Wolff transformation,[44] a decrease in J_{eff}. Although the form of the expression[44] for J_{eff} is unlikely to be valid for *Au*Fe or *Cu*Fe, for which charge-screening considerations

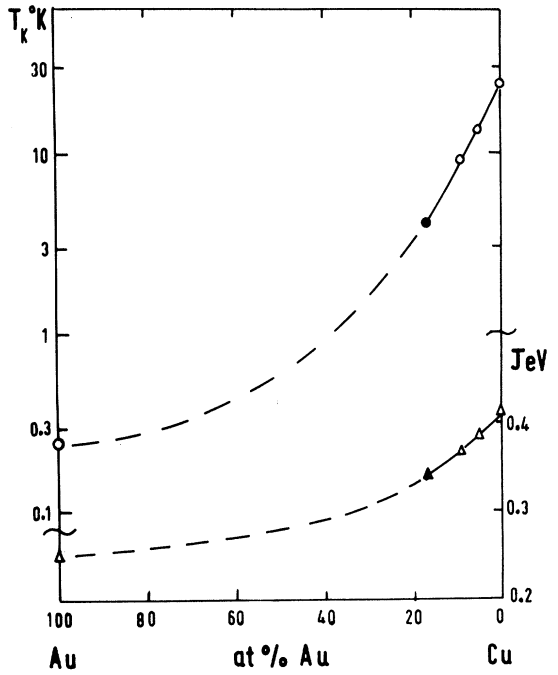

FIG. 17. T_K in °K (○) and J in eV (△) against Au concentration in *CuAu*Fe alloys. The symbols ● and ▲ represent values of T_K and J takes from Ref. 19 for a $Cu_{83}Au_{17}$ (0.02 at. % Fe) alloy.

place the phase shift at E_F for conduction electrons of one spin direction rather close to $\frac{1}{2}\pi$, it is likely that J_{eff} will be very sensitive to the relative positions of this spin band and E_F. Small variations of phase shifts other than $l=2$ across the Cu-Au series will also effect this difference (through the Friedel sum rule) and may lead to the substantial changes in J_{eff} observed.

Examination of Figs. 10, 13, and 16 suggests the existence of a universal dependence of $\Delta\rho$ on T/T_K for $T < T_K$. To determine whether this extends to higher temperatures, we have plotted in Fig. 18 the resistivities of several *CuAu*Fe alloys containing 0, 5, 10, and 100 at. % Au against the reduced temperature T/T_K. As it is in better agreement with values obtained from other properties, we have taken T_K to be 24 °K in the Cu (0.01 at. % Fe) alloys [as found from the fit to Eq. (4b)] rather than 56 °K as obtained from the fit to Eq. (5). We assume, however, that the values of T_K for all of the *CuAu*Fe alloys are in direct proportion to the values obtained from the fit to Eq. (5). Thus, assuming T_K equals 24 °K for Cu (0.01 at. % Fe), then T_K equals 13 and 8.6 °K in the $Cu_{95}Au_5$(0.01 at. % Fe) and $Cu_{90}Au_{10}$(0.08 at. % Fe) alloys, respectively. [The value of 13 °K is in good agreement with the value found from a fit to Eq. (4b) of the $Cu_{95}Au_5$(0.01 at. % Fe) resistivity below 0.8 °K.] The Au(0.0025 at. % Fe) resistivity is also included assuming $T_K = 0.24$. The Hamann function $\frac{1}{2}BF(T)$ with $B = 5.6$ $\mu\Omega$ cm/at. % and $S = 0.77$ is shown by the dashed line. Vertical shifts have been made to bring the curves into coincidence at $T = T_K$. It is clear from the figure that a universal dependence is consistent with the results, provided that reasonable corrections are

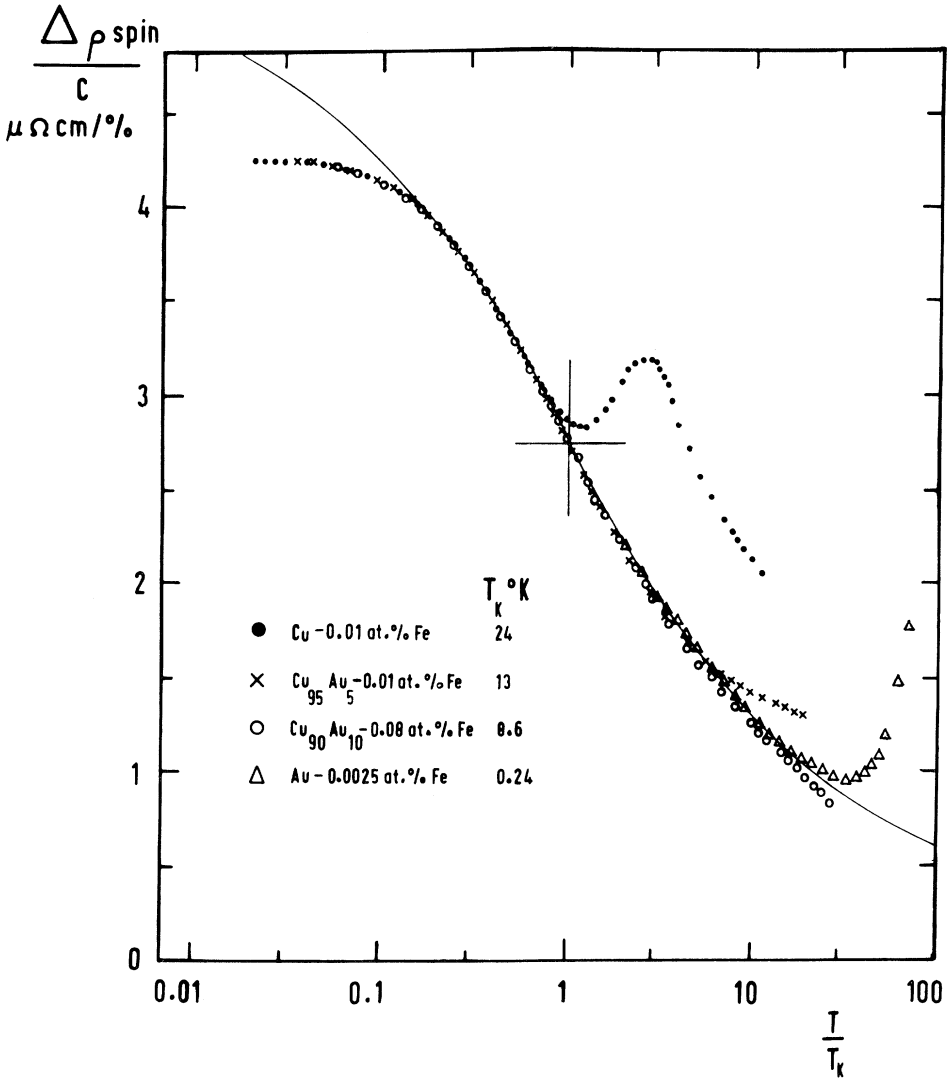

FIG. 18. $\Delta\rho_{spin}/c\mu\Omega$ cm at. % against $\log_{10}(T/T_K)$, for several *CuAu*Fe alloys containing 0, 5, 10, and 100 at. % Au. Full curve represents the Hamann function [Eq. (2)] with $S = 0.77$

made for deviations from Matthiessen's rule.

V. CONCLUSIONS

The following conclusion can be drawn concerning the temperature dependence of the resistance anomaly. For $T \ll T_K$, a parabolic dependence is observed.[45] From Eq. (4b) and the observed step height a value of T_K can be obtained which is in good agreement with values derived from other properties, and which coincides approximately with the temperature at which the curvature $dZ/d\ln T$ is zero. The T^2 dependence is observed over a significantly smaller fraction of T_K ($T/T_K < 0.06$) than is predicted by Nagaoka's expression (4a). At higher temperatures the resistance is well described by the Appelbaum-Kondo expression Eq. (5), though the value of T_K derived is substantially higher than that expected from other properties. The step height E derived from a fit to this expression (Table II) is approximately 1.5 $\mu\Omega$ cm/at. %, and this is substantially smaller than that observed (Fig. 18). At $T > T_K$ the *Au*Fe resistivity (and that of the *CuAu*Fe alloys) is consistent with the Hamann expression (2), though the required value of the spin S is somewhat lower than that derived from susceptibility measurements. A universal dependence on T/T_K is also consistent with the results, with T_K decreasing by two orders of magnitude between *Cu*Fe and *Au*Fe.

Theoretical objections have recently be raised[46] against the Appelbaum-Kondo predictions. The modified theory predicts a finite density of single-particle states at the Fermi surface, and thus, a limiting T^2 dependence to the resistivity, in agreement with the present results and those of Star and Nieuwenhuys[27] on *Cu*Fe. There is thus a measure of agreement between the various theoretical predictions and experimental results in this regime. It should be mentioned, however, that even if a divergent density of states were the correct solution to the idealized problem of the single magnetic impurity in a perfectly periodic potential, it is unlikely that such a divergence could survive in the presence of finite conduction electron mean free paths, residual interactions between impurities, etc., so that a limiting T^2 dependence would always be observed in practice.

ACKNOWLEDGMENTS

We would like to thank Dr. C. E. Johnson, A. E. R. E. Harwell, and the Fulmer Institute for providing the alloys used in the present investigation.

---

†Work sponsored in part by the Air Force Materials Laboratory (AFSC) through the European Office of Aerospace Research (OAR), U.S. Air Force, under Contract No. F61052-68-C-0011.

[1]J. Kondo, Progr. Theoret. Phys. (Kyoto) 32, 37 (1964).

[2]Y. Nagaoka, Phys. Rev. 138, A1112 (1965).

[3]For an extensive theoretical review of the magnetic impurity problem see J. Kondo, in *Solid State Physics*, edited by F. Seitz, D. Turnbull, and H. Ehrenreich (Academic, New York, 1969), Vol. 23.

[4]J. W. Loram, T. E. Whall, and P. J. Ford (unpublished).

[5]K. Kume, J. Phys. Soc. Japan 23, 1226 (1967).

[6]For an excellent experimental and theoretical review, and a comprehensive list of references, see A. J. Heeger, in *Solid State Physics*, edited by F. Seitz, D. Turnbull, and H. Ehrenreich (Academic, New York, 1969), Vol. 23.

[7]A. A. Abrikosov, Physics 2, 5 (1965).

[8]J. A. Appelbaum and J. Kondo, Phys. Rev. Letters 19, 906 (1967).

[9]A. P. Klein, Phys. Letters 26A, 57 (1967).

[10]H. Suhl and D. Wong, Physics 3, 17 (1967).

[11]D. R. Hamann, Phys. Rev. 158, 570 (1967).

[12]M. J. Levine, T. V. Ramakrishman, and R. A. Weiner, Phys. Rev. Letters 20, 1370 (1968).

[13]N. Rivier and M. J. Zuckermann, Phys. Rev. Letters 21, 904 (1968).

[14]J. S. Dugdale and Z. A. Baszinski, Phys. Rev. 157, 552 (1967).

[15]G. K. White, Can. J. Phys. 33, 119 (1955).

[16]B. Knook, thesis, Leiden University, 1962 (unpublished).

[17]M. D. Daybell and W. A. Steyert, Phys. Rev. Letters 18, 398 (1967).

[18]D. K. C. Macdonald, W. B. Pearson, and I. M. Templeton, Proc. Roy. Soc. (London) A266, 161 (1962).

[19]W. M. Star, F. B. Basters, and C. van Baarle, in *Proceedings of the Eleventh International Conference on Low Temperature Physics*, edited by J. F. Allen, D. M. Finlayson, and D. M. McCall (University of St. Andrews Printing Department, St. Andrews, Scotland, 1969), p. 1250.

[20]Specimens 2–13 were prepared by the Fulmer Institute and specimens 14–17 were prepared by the Analytical Division, A. E. R. E. Harwell. Specimen 1 was prepared at a later date in this laboratory. Chemical analyses were performed by Daniel Griffith and Co., London.

[21]W. B. Pearson, *A Handbook of Lattice Spacings and Structures of Metals* (Pergamon, New York, 1967).

[22]Atomic percentages are used throughout.

[23]M. Z. Kohler, Physik 126, 495 (1949).

[24]D. K. C. Macdonald, in *Handbuch der Physik*, edited by S. Flügge (Springer, Berlin, 1956), Vol. 19, p. 146.

[25]T. E. Whall, J. W. Loram, and P. J. Ford (unpublished). Discrepances from this simple relation are observed in the low–residual-resistivity alloys between 50 and 150 °K.

[26]See, for example, K. H. Fischer, in *Proceedings of the Eleventh International Conference on Low Temper-*

ature Physics, edited by J. F. Allen, D. M. Finlayson, D. M. McCall (University of St. Andrews Printing Office, St. Andrews, Scotland, 1969), p. 1239.

[27]W. M. Star and G. J. Nieuwenhuys, Phys. Letters 30A, 22 (1969).

[28]P. E. Bloomfield and D. R. Hamann, Phys. Rev. 164, 856 (1967).

[29]D. J. Scalapino, Phys. Rev. Letters 16, 937 (1966).

[30]C. M. Hurd, J. Phys. Chem. Solids 28, 1345 (1967).

[31]J. W. Loram, A. D. C. Grassie, and G. A. Swallow, Phys. Rev. (to be published).

[32]F. du Chatenier, J. de Nobel, and B. M. Boerstoel, Physica, 32, 561 (1966).

[33]R. J. Potton (private communication).

[34]A. Kjekshus and W. B. Pearson, Can. J. Phys. 40, 98 (1962).

[35]C. M. Hurd, Phys. Rev. Letters 18, 1127 (1967).

[36]J. P. Franck, F. D. Manchester, and D. L. Martin, Proc. Roy. Soc. (London) A263, 494 (1961).

[37]D. C. Golibersuch and A. J. Heeger, Phys. Rev. 182, 584 (1969).

[38]K. Yosida, Phys. Rev. 107, 396 (1957).

[39]W. M. Star and B. M. Boerstoel, Phys. Letters 29A, 26, (1969). Similar concentration-dependent effects have been seen by Star *et al.* in *Cu*Fe and *Pd*Cr.

[40]Y. Nagaoka, J. Phys. Chem. Solids 27, 1139 (1966).

[41]H. Suhl, Solid State Commun. 4, 487 (1966).

[42]J. C. F. Brock, J. C. Ho, G. P. Schwartz, and N. E. Phillips, in *Proceedings of the Eleventh International Conference on Low Temperature Physics*, edited by J. F. Allen, D. M. Finlayson, and D. M. McCall (University of St. Andrews Printing Department, St. Andrews, Scotland, 1969), p. 1229.

[43]M. D. Daybell and W. A. Steyert, Rev. Mod. Phys. 40, 380 (1968).

[44]J. R. Schrieffer and P. A. Wolff, Phys. Rev. 149, 491 (1966).

[45]A Parabolic dependence has also been observed in *Al*Mn and *Al*Cr by A. D. Caplin and C. Rizzuto, Phys. Rev. Letters 21, 746 (1968); also in *Pd*Cr (Ref. 39).

[46]D. R. Hamann and J. A. Appelbaum, Phys. Rev. 180, 334 (1969).

PHYSICAL REVIEW B VOLUME 2, NUMBER 4 15 AUGUST 1970

Exchange Potentials in a Nonuniform Electron Gas

A. W. Overhauser
Scientific Research Staff, Ford Motor Company, Dearborn, Michigan 48121
(Received 17 November 1969)

Off-diagonal matrix elements of the exchange operator are computed for a degenerate electron gas having a small sinusoidal density modulation. The extreme nonlocal character of exchange is shown explicitly by its wave-vector dependence. The Slater exchange approximation severely underestimates the off-diagonal action of the exact exchange operator (by a numerical factor approaching ∞ for long-wavelength modulations). Such errors are largely compensated by neglect of the correlation potential.

In recent years there has been considerable debate[1] on how best to approximate the (nonlocal) exchange operator A with a local potential. A frequent choice is the Slater $\rho^{1/3}$ relation

$$A_S = -3e^2(3\rho/8\pi)^{1/3}\,, \tag{1}$$

where $\rho(\vec{r})$ is the electron density. We believe that an explicit display of the properties of the exact A for a simple case indicates the futility of debate.

Consider a degenerate electron gas having a density

$$\rho(\vec{r}) = \rho_0(1 - p\cos\vec{q}\cdot\vec{r})\,. \tag{2}$$

The mean density is $\rho_0 = k_F^3/3\pi^2$, and the fractional modulation p is assumed small. We shall presume that the modulation is caused by a (total) perturbing potential $V\cos\vec{q}\cdot\vec{r}$. Accordingly, the one electron wave functions are

$$\psi_{\vec{k}} \cong e^{i\vec{k}\cdot\vec{r}}[1 + (V/2\Delta_+)e^{i\vec{q}\cdot\vec{r}} + (V/2\Delta_-)e^{-i\vec{q}\cdot r}]\,, \tag{3}$$

where the energy denominators are $\Delta_+(\vec{k}) \equiv E(\vec{k}) - E(\vec{k}+\vec{q})$, etc. We neglect any $\vec{k}$ dependence of V. These wave functions are the ones generally employed, e.g., in the random-phase approximation (RPA), with or without local exchange and correlation corrections. If we take $E(\vec{k}) = \hbar^2k^2/2m$ and sum $|\psi_{\vec{k}}|^2$ over all occupied states, we find the modulation to be

$$p = (3V/2E_F)g(q/2k_F)\,, \tag{4}$$

where

$$g(x) \equiv \tfrac{1}{2} + [(1-x^2)/4x]\ln\left|(1+x)/(1-x)\right|$$

and $E_F = \hbar^2k_F^2/2m$.

The matrix element of the Slater potential is, from (1) and (2), in the *pure-momentum* represen-